

other reactions catalyzed by palladium²⁵ have lead to the conclusion that the metal atom should be given a large perturbation in order to activate the d^9s^1 state only capable of giving strong bonds with an incoming ligand. The localization of the SOMO of PdClPH₃ on the d metal orbital is indicative of such a promotion of the bonding state. The Mulliken population obtained for palladium in the fragment, $(sp)^{0.36}(d)^{9.28}$, is not quite characteristic however of a d^9s^1 complex. The presence of a phosphine ligand which tends to destabilize the metal bonding orbitals and to favor the d^{10} state^{24a,b} is at the origin of this intermediate situation. The incoming of the nitroxyl ligand achieves the metal activation, evidenced by the rise of the sp population from 0.36e to 0.59e and the concomitant decrease of the overall d population to 8.96e.

The evolution of these populations shows that the resonance between the d^{10} and the d^9s^1 configurations is a key point for describing the energetics of the nitroxyl ligand approach along the reaction path and the bond energy between the two fragments. This would require a careful MCSCF and CI treatment which has not been carried out since this point was beyond the scope of the present study.

(25) (a) Bäckvall, J. E.; Björkman, E. E.; Pettersson, L.; Siegbahn, P. J. *Am. Chem. Soc.* **1984**, *106*, 4369-4373. (b) Bäckvall, J. E.; Björkman, E. E.; Pettersson, L.; Siegbahn, P. *Ibid.* **1985**, *107*, 7265-7267. (c) Bäckvall, J. E.; Björkman, E. E.; Pettersson, L.; Siegbahn, P.; Strich, A. *Ibid.* **1985**, *107*, 7408-7412. (d) Blomberg, M. R. A.; Siegbahn, P. E. M.; Bäckvall, J. E. *Ibid.* **1987**, *109*, 4450-4456.

7. Conclusion

The bonding in CuBr₂TMPO and PdCl(PPh₃)TMPO has been interpreted in terms of the interactions between the π^* and π orbitals of NO on the one hand and the two combinations involving the metal d_{xy} orbitals on the other hand. The balance of these interactions depends on the nature of the SOMO in the bent ML₁L₂ fragment, conditioned itself by the energy of the d levels in the free metal. The low energy of the copper d levels yields for CuX₂ a SOMO with main halogen character. The contribution of this SOMO to the interaction with the NO π^* orbital extends the bonding interactions to the halogen ligands, without any significant change of the NO π^* orbital population. At variance from that, the high energy of the valence d levels of palladium gives rise to a SOMO with major metal character for PdCl(PR₃). This SOMO is higher in energy than the NO π^* orbital, and the interaction of the magnetic orbitals induces some charge transfer from the metal to the nitroxyl radical. This interpretation agrees with the NO distances characterized for the free TMPO radical and for the two complexes investigated in the present study. We expect the synthesis and characterization of other electron-rich nitroxyl complexes with η^2 coordination to help in refining the present analysis.

Acknowledgment. All calculations have been carried out on the CRAY-2 computer of the Centre de Calcul Vectoriel de la Recherche (Palaiseau, France) through a grant of computer time from the CCVR.

Ge-Ge Bonding in the High-Pressure Modification of Lithium Germanide: A Near-Zintl Phase

Paul Sherwood[†] and Roald Hoffmann*

Contribution from the Department of Chemistry and Materials Science Center, Baker Laboratory, Cornell University, Ithaca, New York 14853-1301. Received June 19, 1989

Abstract: The Zintl-phase LiGe has recently been shown to undergo a transformation at elevated temperature and pressure to a metastable modification, which differs markedly from the normal-pressure form in the bonding between the Ge atoms. In the normal form the Ge net is exclusively three-connected, but in the high pressure (HP) form there is a mixture of Ge environments. One-third are approximately tetrahedrally four-connected, while the remainder have two short bonds (to the four-connected atoms) and two longer contacts (to other atoms of the same type), arranged in a distorted square plane. Whether or not the longer contacts are ignored, the HP form no longer obeys the electron-counting principles of Zintl or Klemm. In this paper we examine the bonding between the planar four-coordinated atoms and discuss the way the deviation from the Zintl counting rules can be seen to be consistent with the observed structure.

The Zintl phases¹ are one group of binary materials in which the simplest theories of covalent bonding in molecules have proved most useful. In these compounds the large difference in electronegativity between the two component elements enables a principally ionic model to be used for the distribution of valence electrons between the two atom types A and B; the electropositive atoms A (usually alkali-metal or alkaline-earth elements) are considered to give up their valence electrons to the more electronegative element B (generally from one of the groups 13-16). However, because of the stoichiometries, the resulting anions do not achieve closed-shell (or octet) configurations, as in simple ionic complexes (e.g., NaCl). They are isoelectronic not with the noble gases, but with other p-block elements (e.g., S or P), and so form bonds yielding anionic networks and clusters. The number of bonds expected between the non-metal atoms is easily anticipated from the total valence electron count, including the electrons

donated by the cations.² The cations are distributed among these networks and clusters.

As noted by Schäfer and Eisenmann,³ the Zintl phases may be considered to be intermediate between simple ionic salts and the intermetallic phases. The boundary between phases for which the Zintl concept works well, and those in which there is important metallic bonding between the two components, is not distinct. A number of factors affect the importance of these two types of bonding. Intermetallic character increases as the electronegativity difference between A and B decreases. For a given binary system the intermetallic character also becomes more important as the mole fraction of the electropositive element A increases. This is clearly expected, as in the limit pure A would have a metallic

(1) Zintl, E. *Angew. Chem.* **1939**, *52*, 1.

(2) (a) Mooser, E.; Pearson, W. B. *Phys. Rev.* **1965**, *101*, 1608. (b) Klemm, W. *Proc. Chem. Soc.* **1958**, 329. (c) Busmann, E. Z. *Anorg. Allg. Chem.* **1961**, *313*, 90.

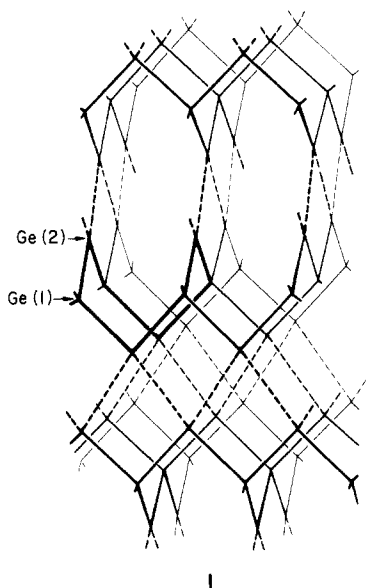
(3) Schäfer, H.; Eisenmann, B. *Rev. Inorg. Chem.*, **1981**, *3*, 29.

[†] Current address: SERC Daresbury Laboratory, Warrington, WA4 4AD, UK.

structure, while pure B would usually be a covalently bound solid. Generally, as either of these factors favoring metallic bonding becomes more important, the Zintl electron-counting scheme fails, and the importance of the covalently bound network or clusters decreases. However, residual covalent bonding between the B atoms persists, often as a result of distortions within a metallic (close-packed) structure. There are also examples of phases, for instance Li_5NaSn_4 ,⁴ that obey the Zintl electron-counting rules, while still containing regions that conform to the α -W type metallic structure.

One example of a phase for which the Zintl concept works well is LiGe .^{5a} The Ge^- ions form a three-connected net, as expected for an ion isoelectronic with phosphorus. In the structure of the Ge network, not shown here, all Ge atoms are equivalent, and each is part of two fused eight-membered rings.

It has recently been reported that LiGe may be transformed, by treatment with 4 GPa of pressure at 500 °C for 10 min, followed by rapid cooling to room temperature, into a metastable high-pressure (HP) phase.^{5b} The structure of the Ge net of the HP phase is shown in 1. It also consists of eight-membered rings,



one of which is shown in bold in 1, but in this case adjacent rings are fused in such a way as to share three atoms, rather than two. The HP network, in contrast to that of the normal-pressure allotrope, has a distinctly layered structure. Within a layer, Ge-Ge separations of 2.70 Å (marked by solid lines) form a two-dimensional net of four-coordinate (pseudotetrahedral) and two-coordinate atoms. These are represented by the atoms labeled Ge(1) and Ge(2) in 1. These layers are stacked, with a repeat unit of four layers, so that the two-coordinate atoms of adjacent layers interact ($\text{Ge}\cdots\text{Ge}$, 3.04 Å, dashed lines). The two long additional bonds thus formed are coplanar with the two short bonds within the layer, giving these Ge(2) atoms distorted square-planar coordination. The Li atoms (not shown in 1) lie at two crystallographically distinct sites—at the centers of the eight-membered rings and alternately above and below the two-coordinate Ge atoms.^{5b}

Although the internuclear separations clearly suggest the presence of a covalently bonded Ge network, the HP LiGe structure does not fit the Zintl model. Neglecting the interlayer interactions, each group of 3 Ge atoms (1 pseudotetrahedral and 2 two-coordinate) would require 16 electrons (4 for each four-coordinate atom, and 6 for the two-coordinate atoms, which must be isoelectronic with O to have closed-shell configurations). The number of electrons actually present is 15. For an electron count of 16e/3Ge we would not expect any interlayer bonding to occur.

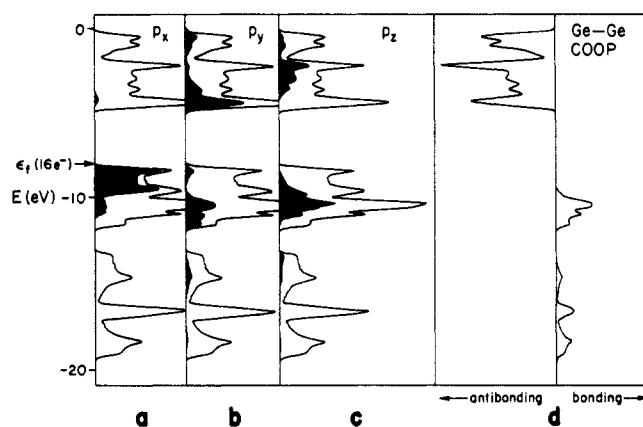


Figure 1. Calculated DOS for the 2D slab 2. The projections (shaded regions) indicate the contributions to this DOS from AOs of (a) p_x , (b) p_y , and (c) p_z type on the Ge atoms on the surface of the slab (for labeling scheme, see text). (d) COOP curve for the Ge-Ge bond.

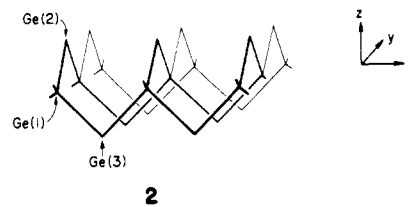
It seems reasonable to assume that the presence of weak interlayer contacts suggested by the structural data and the "electron deficiency" (in the Zintl sense) are related.

What we attempt to do in this paper is examine this relationship. We do so without abandoning the underlying assumption of the Zintl model—that the Li atoms give their valence electrons to the Ge substructure and do not become involved in covalent bonding. We omit the Li atoms from all calculations, while adjusting the electron count to include their valence electrons. The intermetallic contribution to the bonding is thus ignored, even though it is almost certainly important. From the criteria given above, LiGe is expected to lie close to the Zintl-intermetallic borderline, as it is not a Ge-rich phase, and the electronegativity difference between Li and Ge (1.0 vs 1.8) is small compared to most systems that show Zintl behavior. Compression also favors intermetallic bonding.

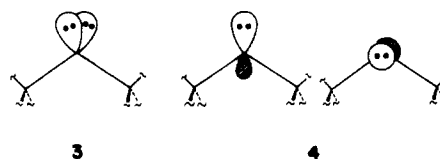
Our approach begins with an examination of the electronic structure of a single Ge layer of the HP LiGe structure. We will then consider the way the interactions between layers are dependent on electron count and try and explain why a stacking pattern that leads to planar 2 + 2 coordinated Ge atoms is adopted.

Electronic Structure of a Germanium Layer

As expected, our extended Hückel calculations (which are described in the Computational Appendix) on a single two-dimensional layer of the HP LiGe structure 2 indicate that it has all the characteristics of a covalently bonded network. For an



electron count of 16 per 3Ge, all bonding and nonbonding crystal orbitals are occupied and there is a substantial band gap. The calculated density of states (DOS) for this system is shown in Figure 1, together with the contributions to this DOS from some atomic orbitals (AOs). Our main interest is the mode of interaction between the two-coordinate atoms, Ge(2) and Ge(3) in 2, and the corresponding atoms in the next layer. For the 16e/3Ge count, the isoelectronic relationship between these atoms and O suggests that these atoms each carry two nonbonding pairs of electrons, as shown in the alternative representations 3 and 4.



(4) Volk, R.; Müller, W. *Z. Naturforsch.* **1978**, *33B*, 593.

(5) (a) Menges, E.; Hopf, V.; Schäfer, H.; Weiss, A. *Z. Naturforsch.* **1969**, *24B*, 1351. (b) Evers, J.; Oehlinger, G.; Sextl, G.; Becker, H.-O. *Angew. Chem.* **1987**, *99*, 69; *Angew. Chem., Int. Ed. Engl.* **1987**, *26*, 76.

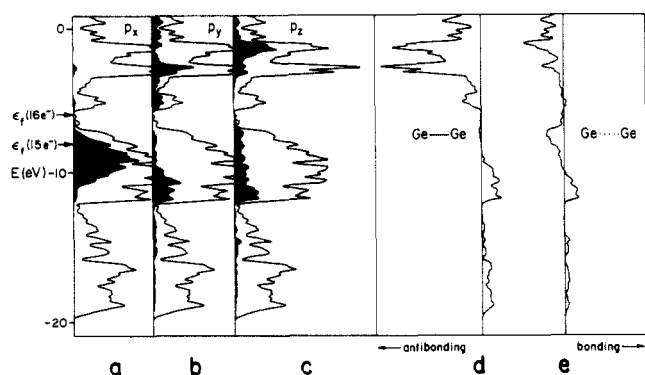


Figure 2. Calculated DOS for the Ge substructure of HP LiGe. The projections (shaded regions) indicate the contributions to this DOS from AOs of (a) p_x , (b) p_y , and (c) p_z type on the planar coordinated Ge atoms (for labeling scheme, see text). COOP curves for (d) the short intralayer Ge-Ge bond, and (e) the long (interlayer) Ge...Ge contacts.

From the projection Figure 1a we can see that the highest occupied states of the layer are composed of Ge p_x character on Ge(2), and p_y on Ge(3). [The symmetry of the net makes Ge(2) p_x equivalent to Ge(3) p_y , and Ge(2) p_y equivalent to Ge(3) p_x ; for brevity we will use from here on the Ge(2) designator, p_x or p_y type, to refer to both Ge(2) and Ge(3).] These orbitals do not interact strongly with each other or with similar orbitals on neighboring unit cells and give rise to a concentration of states close to the Ge p-orbital energy (here -9.0 eV). The other nonbonding pair on Ge(2) is represented by a group of states with slightly lower energy, with predominantly p_z character (Figure 1c). The bottom of the lower p band and the lowest unoccupied states are both composed largely of p_y -type orbitals (Figure 1b) and represent the σ and σ^* orbitals of the Ge network.

The crystal orbital overlap population (COOP) curve (Figure 1d) supports this simple analysis. Clearly the Ge-Ge bonding comes from the low-lying Ge s band, and from the bottom of the p band, while the upper part of the p band (the p_x -type lone pair) is predominantly nonbonding.

Stacking of the Layers

Before proceeding to a discussion of the interlayer bonding, it is worth reiterating that our calculation ignores the Li^+ ions completely. Any quantitative consideration of the energetics of different stacking patterns must include the Li^+ ions—even in the limit of complete charge transfer from Li to Ge electrostatic and packing considerations will be very important.

In the HP solid the layers are arranged such that the two-coordinate Ge atoms have the planar local geometry seen in 1. Figure 2 shows the calculated DOS for the Ge substructure of the HP form, together with the same AO projections as in Figure 1. The filling levels for 16 and 15 electrons per 3Ge unit are marked. The main difference between this DOS and that for a layer is the broadening of the bonding/nonbonding and antibonding p bands. There is no longer a significant band gap for the 16e filling, and the filling level for the observed count of 15e lies well inside the DOS envelope of the bonding and nonbonding p states. Thus we might expect the Ge network alone of the HP form to show some metallic properties.

Comparison of the DOS projections with Figure 1 reveals that the largest changes concern states with significant p_z character on the two-coordinate atoms. The p_z character now persists up to the 16e/3Ge filling point. The COOP curve for the intralayer (short) Ge-Ge bond is similar in form to the corresponding curve for the layer (Figure 1d), except for one feature—there is considerable Ge-Ge antibonding character in a group of crystal orbitals at around -5 eV, considerably lower in energy than the bottom of the Ge-Ge antibonding band in Figure 1. We will return to this later; it is sufficient to note that as these states are unoccupied there is little effect on the bonding.

The COOP curve for the longer interlayer Ge...Ge bonds (Figure 2e) is more interesting. It reveals that the orbitals at the bottom of the bonding/nonbonding p band contribute bonding

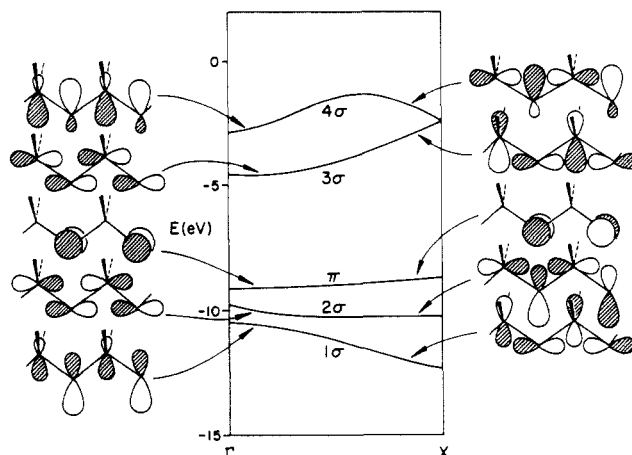


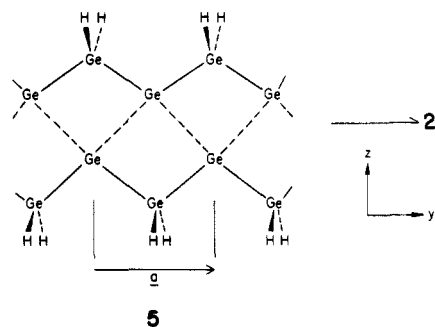
Figure 3. Calculated band structure for the 1D chain $(\text{Ge}_2\text{H}_2)_\infty$ with an indication of the nature of the bands at Γ and X.

character to the interlayer contacts, while those at the top (up to the filling level of 16e) are antibonding to a similar degree. For the 16e filling there will be no net bonding between the layers, but for lower electron counts, such as that observed, net bonding is expected. This is supported by the computations; we calculate net overlap populations of 0.519 (Ge-Ge) and 0.154 (Ge...Ge) for the observed geometry and band filling.

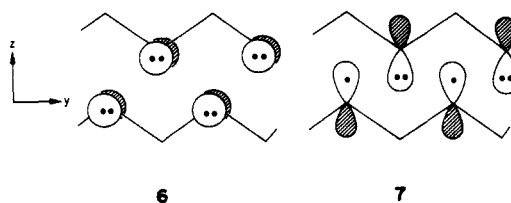
In order to discuss the nature of this net interlayer bonding in orbital terms we turn from the full structure, which has a complicated band structure as a result of its large unit cell, to a simpler 1D model. We can do this because communication between one interlayer bonding zone and the next (i.e., the top and bottom of a given layer) is likely to be small. Different two-coordinate Ge atoms are involved, and they are connected, via the tetrahedral Ge atoms, by what appear to be simple Ge-Ge single bonds.

A One-Dimensional Model

The model we have chosen has the form of a ribbon and is shown in 5. The missing bonds (relative to the HP structure)



have been tied off with hydrogen atoms. The unit cell of this system, as indicated above, contains four Ge atoms, and must carry a charge of -3 to produce the right pattern of nonbonding electrons on the two-coordinate germanium atoms—for each pair of two-coordinate Ge atoms there must be seven nonbonding electrons. Four of these can be considered to reside in p_x orbitals perpendicular to the ribbon plane, 6, while the remaining three incompletely fill the p_z -type orbitals 7. We will start our analysis with



an even simpler model system, half of the ribbon 5. The band structure of this system (Figure 3) illustrates the energies and dispersion of the bands in the absence of the long Ge...Ge contacts. The orbitals at the edges of the Brillouin zone are also shown in

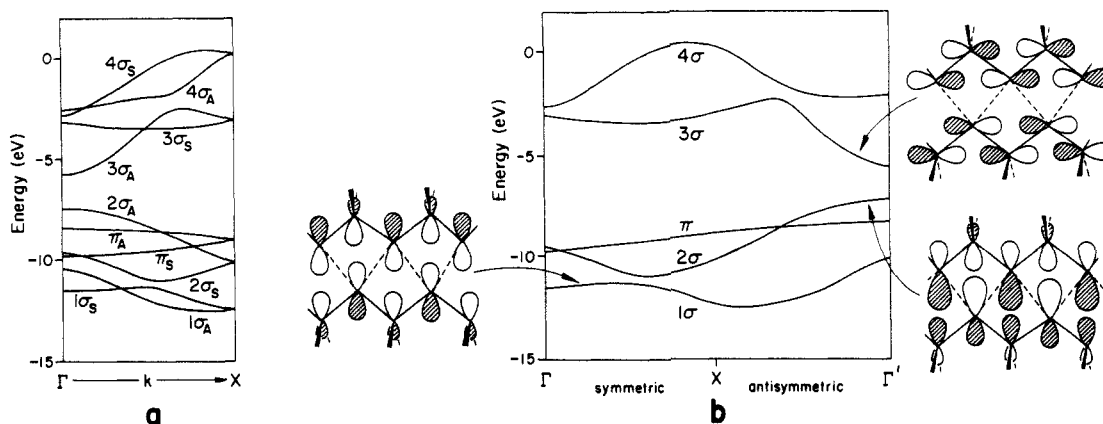


Figure 4. (a) Calculated band structure for the 1D chain $(\text{Ge}_4\text{H}_4)_\infty$. (b) The same band structure "unfolded" about X. The nature of the bands at Γ is indicated.

the figure. Note that there are three other filled, low-lying bands not shown in Figure 3, which have predominantly Ge s character. The nonbonding band made up of the p_x orbitals 6 perpendicular to the ribbon is labeled π . All remaining crystal orbitals are symmetric with respect to this plane and in the interior of the zone have the same symmetry. There is an avoided crossing between bands 1σ and 2σ , the nonbonding p_x character being present in 1σ at the center (Γ) of the Brillouin zone, and in 2σ at the edge (X). Bands 3σ and 4σ are Ge-Ge antibonding.

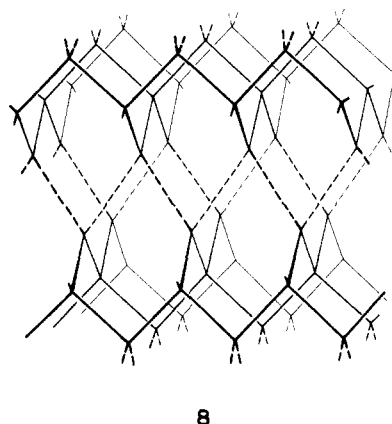
When two such chains are brought together with a long Ge...Ge contact of 3.04 Å, the resulting band structure is as shown in Figure 4a. There are twice as many bands as before, and we have added a symmetry element; a 2_1 screw axis along the ribbon direction. The orbitals in the zone interior are now classified according to this symmetry element also. It can be seen that each band in Figure 3 gives rise to two in Figure 4a, one of each symmetry with respect to the screw axis. This symmetry makes it possible to simplify the appearance of Figure 4a by "unfolding" the band structure about X ($k = \pi/a$), so that all bands that are antisymmetric with respect to the screw axis appear to the right of this point, as shown in Figure 4b. A similar analysis of the band structure of ribbon-type systems characterized by 2_1 screw symmetry has been presented by one of us before.⁶

Our discussion of the weak Ge...Ge bonding centers on the fate of the nonbonding electrons shown in 6 and 7. The p_x orbitals form a narrow band (π in Figure 4b) with an energy very similar to the corresponding band in Figure 3, indicating that as expected, interaction between these orbitals is weak. This is not true for the p_y -type orbitals. In Figure 3 they form a relatively flat band, with 1σ at Γ , but 2σ at X due to the avoided crossing. In Figure 4b they form a band (1σ at Γ , 2σ at Γ') with considerable dispersion. The orbital drawings at the zone boundaries show how the orbitals at the bottom of this band are bonding between the two $(\text{Ge}_2\text{H}_2)_\infty$ chains, while those at the top are strongly antibonding. Thus, an electron count that completely fills this band (that corresponding to a $16e/3\text{Ge}$ count in the full structure) will not give rise to any net bonding. However, removal of electrons from the top of this band will lead to bonding between the chains.

Another feature of Figure 4b deserves comment. It can be seen that the lowest Ge-Ge (intrachain) antibonding orbital (3σ , near Γ') is lower in energy (by ~ 1.5 eV) than the lowest Ge-Ge antibonding band in Figure 3. It is clear from the relative phases of the p_y contributions of the band 3σ at Γ in Figure 3 that strong overlap is possible with a similar band on the other 1D chain, and it is this that gives rise to the stabilization at Γ' in Figure 4b. This effect offers an explanation for the appearance of low-lying Ge-Ge antibonding bands in the DOS of the HP Ge substructure in Figure 2, as noted above.

As already emphasized, without consideration of the Li^+ ions we cannot approach the relative energetics of alternative Ge

substructures. However, it is worth considering, for comparison, what Ge...Ge bonding might be available in one alternative stacking pattern of the 2D Ge layers 2, one in which all Ge atoms are in distorted tetrahedral environments. This stacking pattern is shown in 8.



The reader may recognize this structure from its topology; if the layers are brought together to the point that the Ge-Ge separation between the layers is equal to that within the layers, and the Ge atoms are given tetrahedral symmetry, this is the structure of cubic diamond. The fully bonded carbon structure is, of course, characterized by a much lower electron count than that observed here, $12e/3\text{Ge}$.

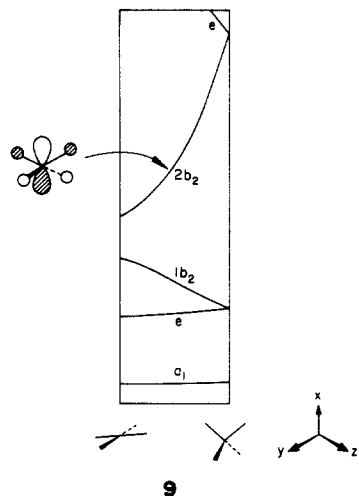
We performed a calculation to compare the Ge...Ge bonding in this "expanded diamond" structure (Ge...Ge, 3.04 Å) with that in 1. The electron count is that appropriate to the LiGe formulation. Although the overlap populations for the short Ge-Ge bonds are similar in the two stacking arrangements (0.515 in 8 vs 0.519 in 1), interlayer bonding is absent in 8 (Ge...Ge overlap populations, -0.015 in 8 vs 0.154 in 1). The substructure 8 also has a higher total energy. The differences can be traced to the filling levels of those bands with interlayer bonding and antibonding character. Stacking 1 allows $2e$ per (two + two)-coordinated Ge to fully occupy bands that contribute little to the interlayer overlap populations, (analogous to π in Figures 3 and 4b), leaving the remaining electrons to $3/4$ -fill 3D versions of the 2σ band of Figure 4b. In structure 8 both p_x and p_z orbitals on the (two + two)-coordinate Ge atoms overlap to form bands (representation 3 for the nonbonding electrons is useful here), and all resulting bands will be filled to around the $7/8$ point. At this filling level the bonding effects of the lower lying crystal orbitals are just canceled out by the antibonding effects of the higher levels.

To put it another way, the diamond structure efficiently partitions half of its orbitals (bands) into strongly bonding ones, half into antibonding ones. It is then ideal for filling half of the bands, the bonding ones, but is destabilizing as one moves past the four electron per center count of carbon.

(6) Hoffmann, R.; Minot, C.; Gray, H. B. *J. Am. Chem. Soc.* **1984**, *106*, 2001.

Although the bonding between the two-coordinate Ge atoms that arises from the partial filling of the 2σ band in Figure 4b has been discussed in the language of extended systems, it is useful to make an analogy with the phenomenon of hypervalency in molecules.

When the coordination sphere of a main-group atom is associated with more than eight electrons, the favored geometry switches from the tetrahedron to a planar arrangement. The origin of this is clear from the Walsh diagram 9 for a D_{4h} to T_d distortion of GeH_4 .⁷ For valence electron counts greater than eight the

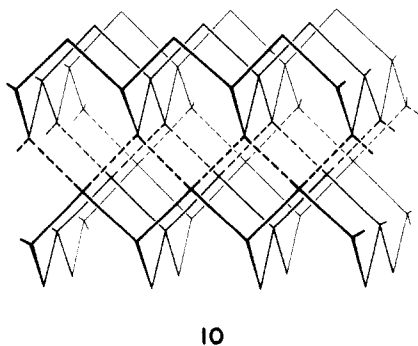


stabilization of the $2b_2$ (p) orbital lowers the energy of the planar structure. It is rather difficult to decide which electron count for GeH_4 makes the bonding most analogous to that in the solid, since in the latter there are "hypervalent" Ge atoms at both ends of the long Ge...Ge bonds. However, as expected from the model band structures discussed above, and confirmed by a Mulliken population analysis, the occupations of the p_x -type orbitals in the solid are close to two. The calculated value (1.79) can be compared with 0.97 for the p_z - and 0.86 for the p_y -type orbitals.

Some Hypothetical Structures Based on the HP LiGe Net

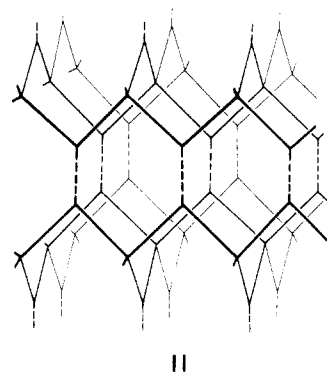
The simple 2D network 2 forms the basis for both the HP LiGe structure and the structure of cubic diamond. It is interesting to consider a few of the many possible structures that might be generated by combining these 2D slabs in other ways.

The simplest variation is perhaps a mixture of the stacking patterns seen in HP LiGe and diamond, in which some interactions between the slabs are of the HP LiGe type, while some are of the diamond type. A large number of structures with large unit cells could be generated this way, which might be observed for systems that have electron counts intermediate between 12 and 15 electrons per 3 framework atoms. A more intriguing possibility is shown in 10; here the stacking pattern results in pseudotetrahedral co-



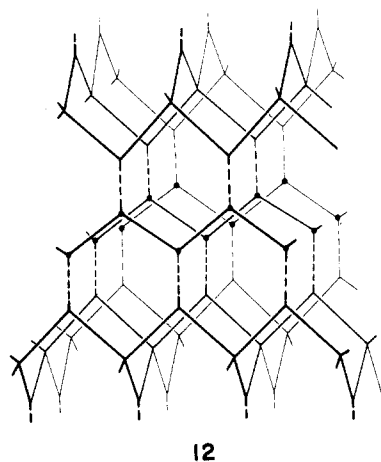
ordination for atoms on the surface of one of the slabs, and distorted square planar for those on the other. Another way of

stacking the layers is shown in 11. This differs from that in the

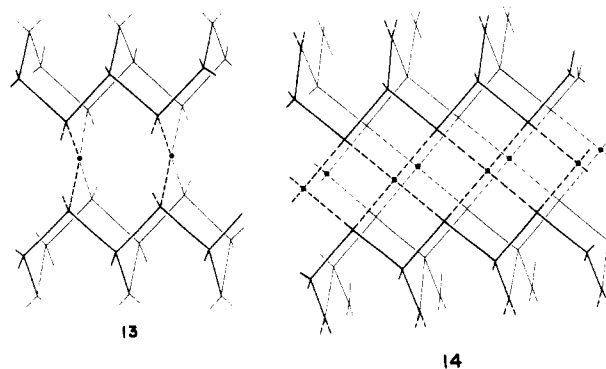


HP LiGe structure by a relative translation of one sheet by half a unit cell with respect to the other, resulting in trigonal coordination for the atoms on the surface of the layers. The interactions between p_x -type orbitals on trigonal atoms belonging to neighboring slabs will be stronger than those in the LiGe network, as a result of a π -type overlap, and we would expect such a system to have an electron count similar to that of diamond (or more relevantly, graphite) so that the bands with π^* character may remain empty.

Further possibilities emerge if we consider the addition of layers of atoms between the slabs 2. One way in which this might occur is shown in 12. The atoms on the surface of the slabs retain their

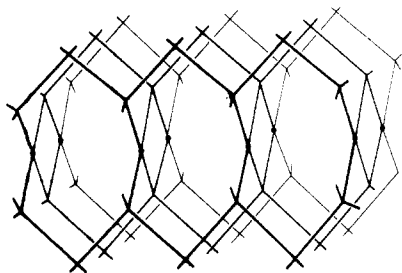


trigonal coordination, but are now linked by bonds of σ and π character to the interleaved atoms, which are sp^2 hybridized as in graphite. If the additional atoms have planar four-fold coordination, we can generate structures 13 and 14. In 13 the atoms



on the surface of the slab 2 have tetrahedral coordination, whereas in 14 they are planar. Finally, we illustrate one possibility, 15, in which the layers 2 are fused together by sharing surface atoms, which consequently have a planar (D_{2h}) coordination. Fusing the layers so that the shared atoms are tetrahedral is just another way

(7) Albright, T. A.; Burdett, J. K.; Whangbo, M. H. *Orbital Interactions in Chemistry*; Wiley-Interscience: New York, 1985.



15

of deriving the cubic diamond structure from 2.

Conclusion

We hope we have demonstrated how the non-Zintl electron count of the HP LiGe structure is related to the presence of weak Ge...Ge bonding and the distorted square-planar geometry for $2/3$ of the Ge atoms seen in the structure. The amount of covalent interlayer bonding is small, and the layers are probably largely held together by ionic forces involving the Li^+ ions. However,

such bonding is greater in the observed structure than in an alternative structure in which all Ge atoms have distorted tetrahedral geometries, for the same reasons that hypervalent $(10e)$ AH_4 complexes adopt planar structures. We think that some of the hypothetical variants described in the last section will not remain unsynthesized for long.

Computational Appendix

All calculations are of the extended Hückel method, using the tight-binding model for extended systems. The parameters used for Ge^8 ($2s$, $H_{ii} = -16.0$ eV, $\zeta = 2.16$; $2p$, $H_{ii} = -9.00$ eV, $\zeta = 1.85$) and H^9 ($1s$, $H_{ii} = -13.6$ eV, $\zeta = 1.30$) were taken from previous work. For the calculation of properties averaged over the Brillouin zone (total energies, DOS and COOP curves) special k-point sets chosen by the method of Ramirez and Böhm¹⁰ were used. These sets assumed tetragonal symmetry, and contained 15 points for the 3D systems and 55 points for the 2D Ge layer.

(8) Thorn, D. L.; Hoffmann, R. *Inorg. Chem.* **1978**, *17*, 126.

(9) Hoffmann, R. *J. Chem. Phys.* **1963**, *39*, 1397.

(10) Ramirez, R.; Böhm, M. C. *Int. J. Quantum Chem.* **1986**, *30*, 391.

Reactions of Butadiene in Zeolite Catalysts by in Situ Variable-Temperature Solid-State Nuclear Magnetic Resonance Spectrometry

Benny R. Richardson, Noel D. Lazo, Paul D. Schettler,[†] Jeffery L. White, and James F. Haw*

Contribution from the Department of Chemistry, Texas A&M University, College Station, Texas 77843. Received May 30, 1989

Abstract: The mechanisms by which butadiene oligomerizes in acidic zeolite catalysts leading to deactivation by pore blockage have been elucidated by using in situ ^{13}C solid-state NMR spectroscopy with magic-angle spinning (MAS). Butadiene is found to oligomerize primarily by the 1,4-addition reaction upon adsorption at its melting point (164 K). Secondary reactions of the oligomers are strongly dependent upon the properties of the zeolite. The initially formed linear product undergoes cyclization reactions to form fused rings in zeolite HY, but isolated rings are formed in the smaller channels of zeolite HZSM-5. Branching reactions and/or 1,2 enchainment result in an appreciable methyl group content in the oligomers formed in zeolite HY. These results provide insight into the mechanisms by which oxide catalysts are deactivated by pore blockage. Neither carbenium ions nor any other reactive intermediates were observed spectroscopically, presumably because such intermediates reacted with either free butadiene or the oligomers so rapidly as to preclude a detectable steady state concentration. A novel experimental procedure for in situ MAS NMR studies of chemical reactions in heterogeneous catalysis is described. This procedure is useful for adsorbates which are too reactive and/or insufficiently volatile for the recently reported CAVERN experiment.

The reactions of hydrocarbons and other adsorbates within zeolite catalysts are of great interest. Traditionally, such reactions are studied by making inferences based on the volatile product distribution or on spectroscopic data obtained following external sample treatment.¹ With the development of high resolution ^{13}C magic-angle spinning (MAS) NMR spectroscopy of solids,² the observation of such reactions in situ has become a realistic goal, especially if variable-temperature methods³ are employed. Recently, this laboratory reported an in situ study of the reactions of propene on the solid-acid catalyst zeolite HY.⁴ In that investigation, a novel sample preparation chamber called the CAVERN (cryogenic adsorption vessel enabling rotor nestling) was used to adsorb the olefin on the catalyst and seal the sample in an MAS rotor at temperatures sufficiently low to prevent the onset of reaction. Sealed rotors prepared in the CAVERN were then

transferred to a precooled MAS NMR probe, and chemical reactions in the zeolite channels were induced by a stepwise temperature ramp. Parallel experiments with ^{13}C labels in different positions (i.e., different isotopomers of propene) showed that label scrambling did not occur and allowed the reaction mechanism to be elucidated.

Conjugated dienes such as butadiene are expected to be considerably more reactive than simple olefins such as propene and are, therefore, expected to be particularly challenging adsorbates for in situ studies of reactions on heterogeneous catalysts. Furthermore, the reactions of dienes on acidic zeolites and related

(1) Anderson, M. W.; Klinowski, J. *Nature* **1989**, *339*, 200.

(2) For reviews of the CP/MAS NMR technique, see: (a) Yannoni, C. S. *Acc. Chem. Res.* **1982**, *15*, 210. (b) Maciel, G. E. *Science (Washington, D. C.)* **1984**, *226*, 282.

(3) Haw, J. F. *Anal. Chem.* **1988**, *60*, 559A.

(4) Haw, J. F.; Richardson, B. R.; Oshiro, I. S.; Lazo, N. D.; Speed, J. A. *J. Am. Chem. Soc.* **1989**, *111*, 2052.

* Author to whom correspondence should be addressed.

[†]Permanent address: Department of Chemistry, Juniata College, Huntingdon, PA 16652.